



PERGAMON

International Journal of Plasticity 15 (1999) 551–574

---

---

INTERNATIONAL JOURNAL OF  
**Plasticity**

---

---

# Effect of material parameters on shear band spacing in work-hardening gradient dependent thermoviscoplastic materials

L. Chen, R.C. Batra\*

*Department of Engineering Science and Mechanics, (MC 0219), Virginia Polytechnic Institute and State University, Blacksburg, VA 24061, USA*

Received in revised form 20 November 1998

---

## Abstract

We study thermomechanical deformations of a viscoplastic body deformed in simple shear. The effect of material elasticity is neglected but that of work hardening, strain-rate hardening, thermal softening, and strain-rate gradients is considered. The consideration of strain-rate gradients introduces a material characteristic length into the problem. A homogeneous solution of the governing equations is perturbed at different values  $t_0$  of time  $t$ , and the growth rate at time  $t_0$  of perturbations of different wavelengths is computed. Following Wright and Ockendon's postulate that the wavelength of the dominant instability mode with the maximum growth rate at time  $t_0$  determines the minimum spacing between shear bands, the shear band spacing is computed. It is found that for the shear band spacing to be positive, either the thermal conductivity or the material characteristic length must be positive. Approximate analytical expressions for locally adiabatic deformations of dipolar (strain-rate gradient-dependent) materials indicate that the shear band spacing is proportional to the square-root of the material characteristic length, and the fourth root of the strain-rate hardening exponent. The shear band spacing increases with an increase in the strain hardening exponent and the thermal conductivity of the material. © 1999 Elsevier Science Ltd. All rights reserved.

*Keywords:* Strain-rate gradient-dependent plasticity; Dominant growth rate; Material characteristic length; Stability

---

## 1. Introduction

Nesterenko et al. (1995) investigated the initiation and propagation of shear bands during the radial collapse of a thick-walled cylinder deformed at a strain-rate of

---

\*Corresponding author.

approximately  $10^4/s$ . They found that twenty shear bands spaced about 1 and 0.85 mm apart formed respectively in titanium and stainless steel cylinders; the estimated values of the maximum shear strain were 0.22 and 0.4, respectively, in titanium and stainless steel. Grady and Kipp (1987) studied simple shearing deformations of a thermally softening rigid plastic material and determined the shear band spacing by accounting for the momentum diffusion due to unloading within a shear band. Wright and Ockendon (1996) also accounted for strain-rate hardening of the material, perturbed the time-dependent homogeneous solution of the governing equations, derived equations linear in the amplitude of the perturbations, and studied the stability of the homogeneous solution. Linear perturbation analysis has been used to study the initiation of material instability by Clifton (1980), Bai (1982), Burns (1985), Molinari (1985) and Anand et al. (1987) amongst others (e.g. see Bai and Dodd, 1992). Wright and Ockendon (1996) postulated that, in an infinite body, perturbations growing at different sites will never merge and result in multiple shear bands. Thus the wavelength of the dominant instability mode with the maximum initial growth rate will determine the shear band spacing. Molinari (1997) has extended Wright and Ockendon's (1996) work to strain-hardening materials and has estimated the error in the shear band spacing due to the finite thickness of the block deformed in simple shear. Batra and Chen (1999) have considered the effects of strain-rate gradients, corresponding higher-order stresses in both the balance laws and the material models, and three constitutive relations, viz. the power law, the Wright–Batra (1987) relation and the Johnson–Cook (1983) relation. They followed Molinari's (1997) approach and defined the shear band spacing as the minimum of  $2\pi/\xi_m(t_0)$  for  $t_0 \geq 0$  where  $t_0$  is the time when the homogeneous solution is perturbed and  $\xi_m$  equals the wave number corresponding to the maximum growth rate at time  $t_0$  of the perturbation. They considered generalizations to gradient-dependent materials of three constitutive relations, viz. the power law studied by Molinari (1997), the Wright–Batra (1987) relation and the Johnson–Cook (1983) relation. In each case the effective stress is maximum at time  $t = 0$ . It was found that for the power law, perturbations introduced just after the effective stress becomes maximum determine the shear band spacing. However, for the other two relations in which thermal softening is modeled by an affine function of temperature, perturbations introduced at a rather large value of  $t_0$  determine the shear band spacing. Molinari (1997) has shown that the strain-hardening of the material can significantly influence the shear band spacing in simple materials. Here we investigate the effect of work hardening in gradient-dependent thermoviscoplastic materials modeled by a power law. As in the previous work of Batra and Chen (1999) we include the effect of strain-rate gradients, and the corresponding higher-order stresses in both the balance laws and the constitutive relations. Molinari's (1997) hardening of the material caused by plastic deformations depended upon the plastic strain, in the present model it depends upon the plastic work done. Kwon and Batra (1988) also considered the effect of material elasticity, perturbed a solution of the nonlinear coupled partial differential equations by introducing a temperature perturbation represented by a cosine wave with twenty cusps, and numerically solved the resulting nonlinear initial-boundary-value problem. They

found that for a typical hard steel modeled as a nonpolar (no strain-rate gradient effects) material, a shear band formed at each trough in the cosine wave in a specimen deformed at an overall strain-rate of 500/s but at each crest when the nominal strain-rate equalled 50,000/s. For dipolar materials with material characteristic length equal to 0.5% of the specimen thickness, at a nominal strain-rate of 500/s a shear band formed only at the two bounding surfaces where the velocity was prescribed and at each crest when the nominal strain-rate equalled 50,000/s. Both for dipolar and nonpolar materials deformed at an average strain-rate of 50,000/s, the distance between adjacent shear bands was found to be 0.258 mm. They did not attempt to find the minimum spacing between adjacent shear bands.

We note that the consideration of strain-rate gradients introduces a material characteristic length,  $\ell$ , in the problem. Batra (1987) and Batra and Kim (1990) have investigated the effect of  $\ell$  on the initiation, growth and band-width of shear bands in heat-conducting thermoviscoplastic materials deformed in simple shear. Batra and Hwang (1994) have studied the same problem for plane strain deformations of thermoviscoplastic materials. Whereas we consider the effect of higher-order stresses in both the balance laws and the constitutive relations, other approaches (e.g. see Aifantis, 1984) have been proposed in which strain gradients are included in the yield function only. Faciu and Molinari (1996, 1998) have incorporated higher-order strain gradients in the relaxation function of Maxwell's rate-type constitutive equation and determined critical wave lengths for the onset of instability and pattern formation. Batra (1975) considered higher-order gradients of temperature and for rigid heat conductors found constitutive relations compatible with the Clausius–Duhem inequality. He showed that thermal disturbances can propagate with finite speed in such materials.

The present work indicates that when the value of the material characteristic length is increased from 0 to 0.025 mm, the shear band spacing in an infinite block of 1018CR steel deformed in simple shear increases from 1.05 to 3.4 mm. Molinari's estimate for the effect of the finite thickness of the block suggests that these values could deviate by about 21%—thus bringing them closer to the observed value of approximately 1 mm.

## 2. Formulation of the problem

Neglecting the effects of material elasticity, equations governing the thermo-mechanical deformations of a strain-hardening, gradient-dependent, homogeneous and isotropic thermoviscoplastic layer deformed in simple shear are (e.g. see Wright and Batra (1987))

$$\rho \dot{v} = (s - \ell \sigma_{,y})_{,y}, \quad (1)$$

$$\dot{\theta} = k \theta_{,yy} + s v_{,y} + \ell \sigma v_{,yy}, \quad (2)$$

$$\sigma v_{,y} = \ell s v_{,yy}, \quad (3)$$

$$\dot{\psi} = (sv_{,y} + \ell\sigma v_{,yy}) / \left(1 + \frac{\psi}{\psi_0}\right)^n, \quad (4)$$

$$I \equiv (v_{,y}^2 + \ell^2 v_{,yy}^2)^{1/2} = f(s, \sigma, \theta, \psi). \quad (5)$$

These equations are written in nondimensional variables for a layer bounded by the planes  $y = \pm 1$  and being sheared in the  $x$ -direction. Here  $v$  is the present velocity of a material particle in the direction of shearing, a superimposed dot indicates the material time derivative, and a comma followed by  $y$  signifies partial differentiation with respect to  $y$ . Variables  $\rho, s, \sigma, \theta, k, \psi$  and  $\ell$  denote, respectively, the mass density, the shear stress, the dipolar stress corresponding to the kinematic variable  $v_{,yy}$ , the temperature, thermal conductivity, work-hardening parameter and the material characteristic length. Eqs. (1) and (2) are respectively the balance of linear momentum, and the balance of internal energy, and Eqs. (3)–(5) are the constitutive relations when elastic deformations are neglected. Eq. (4) signifies that the rate of work hardening is proportional to plastic working, and in Eq. (2) all of the plastic working is assumed to be converted into heating. If  $\psi$  is interpreted as the effective plastic strain, and  $\sigma_e = (s^2 + \sigma^2)^{1/2}$  as the effective stress, then  $\sigma_e = \left(1 + \frac{\psi}{\psi_0}\right)^n$  represents the effective stress vs the effective plastic strain curve in quasistatic deformations of the body. Eq. (5) describes the thermoviscoplastic response of the material. The governing equations for nonpolar materials are obtained from Eqs. (1)–(5) by setting  $\ell = 0$ . The non-dimensional variables are related to their dimensional counterparts (denoted below by a superimposed hat) as follows.

$$\begin{aligned} \hat{y} &= Hy, \hat{\ell} = H\ell, \hat{\psi} = \psi, \hat{s} = \kappa_0 s, \hat{\sigma} = \kappa_0 \ell \sigma, \\ \hat{t} &= t/\dot{\gamma}_0, \hat{\theta} = \theta_r \theta, \rho = \hat{\rho} H^2 \dot{\gamma}_0^2 / \kappa_0, k = \hat{k} / (\hat{\rho} \hat{c} \dot{\gamma}_0 H^2), \theta_r = \frac{\kappa_0}{\hat{\rho} \hat{c}}. \end{aligned} \quad (6)$$

Here  $2H$  equals the thickness of the layer,  $\kappa_0$  is the yield stress of the material in a quasistatic simple shear test,  $\dot{\gamma}_0$  is the average strain-rate, and  $\hat{c}$  is the specific heat.

We postulate the following form for the function  $f$  in Eq. (5).

$$f(s, \sigma, \theta, \psi) = \mu_0^{-\frac{1}{m}} \theta^{-\frac{v}{m}} \left(1 + \frac{\psi}{\psi_0}\right)^{-\frac{m}{m}} (s^2 + \sigma^2)^{\frac{1}{2m}}. \quad (7)$$

Here  $\mu_0$  is a strength parameter,  $m$  describes the strain-rate hardening of the material, and  $v$  its thermal softening. The relation between nondimensional  $\mu_0$  and dimensional  $\hat{\mu}_0$  is

$$\mu_0 = \frac{\dot{\gamma}_0^m \kappa_0^{v-1}}{(\hat{\rho} \hat{c})^v} \hat{\mu}_0. \quad (8)$$

A homogeneous solution of Eqs. (1)–(5) and (7) under the boundary conditions

$$\theta_{,y}|_{y=\pm 1} = 0, v|_{y=\pm 1} = 1, \tag{9}$$

is

$$\bar{s} = \begin{Bmatrix} \bar{v} \\ \bar{s} \\ \bar{\sigma} \\ \bar{\theta} \\ \bar{\psi} \end{Bmatrix} = \begin{Bmatrix} \mu_0(\tilde{\psi}_0)^{\tilde{n}}(\bar{\theta})^{v+\tilde{n}} \\ 0 \\ [\theta_i^{\hat{n}-v} + t(\hat{n}-v)\mu_0(\tilde{\psi}_0)^{\tilde{n}}]^{1/(\hat{n}-v)} \\ \psi_0((\tilde{\psi}_0)^{\hat{n}}(\bar{\theta})^{\hat{n}} - 1) \end{Bmatrix}, \tag{10}$$

where

$$\tilde{\psi}_0 = \frac{(1+n)}{\psi_0}, \tilde{n} = \frac{n}{1+n}, \hat{n} = \frac{1}{1+n} = 1 - \tilde{n}, \theta_i \equiv \bar{\theta}(0) = \left(1 + \frac{\bar{\psi}(0)}{\psi_0}\right)^{1+n} / \tilde{\psi}_0, \tag{11}$$

$\theta_i$  and  $\bar{\psi}(0)$  are respectively the values of the homogeneous solutions  $\bar{\theta}$  and  $\bar{\psi}$  at time  $t = 0$ . When  $\theta_i$  and  $\bar{\psi}(0)$  are not related by (11)<sub>4</sub>, which is generally the case, then a homogeneous solution of Eqs. (1)–(5), (7) and (9) is

$$\bar{s} = \begin{Bmatrix} \bar{v} \\ \bar{s} \\ \bar{\sigma} \\ \bar{\theta} \\ \bar{\psi} \end{Bmatrix} = \begin{Bmatrix} \mu_0\bar{\theta}^v \left(1 + \frac{\bar{\psi}}{\psi_0}\right)^n \\ 0 \\ \theta_i + \left[ \left(1 + \frac{\bar{\psi}}{\psi_0}\right)^{n+1} - \left(1 + \frac{\bar{\psi}(0)}{\psi_0}\right)^{n+1} \right] / \tilde{\psi}_0 \\ \bar{\psi} \end{Bmatrix} \tag{12}$$

and  $\bar{\psi}$  is found numerically by simultaneously solving  $\dot{\bar{\theta}} = \dot{\bar{\psi}} \left(1 + \frac{\bar{\psi}}{\psi_0}\right)^n, \dot{\bar{\psi}} = \mu_0\bar{\theta}^v$ . Henceforth we work with the homogeneous solution given by Eq. (12).

### 3. Perturbation analysis

Consider an infinitesimal perturbation of the homogeneous solution at time  $t = t_0$ . That is, let

$$\delta s(y, t, t_0) = e^{\eta(t-t_0)} e^{i\xi y} \delta s^0, t \geq t_0, \tag{13a}$$

where

$$\delta s^0 = [\delta v^0, \delta s^0, \delta \sigma^0, \delta \theta^0, \delta \psi^0]^T, \tag{13b}$$

is a small disturbance in the homogeneous solution. Here  $\xi$  is the wave number and  $\eta$  its initial growth rate.  $Re(\eta) < 0$  implies that the homogeneous solution is stable at time  $t_0$ , and  $Re(\eta) > 0$  means that it is unstable.

Substitution of

$$\mathbf{s}(y, t, t_0) = \bar{\mathbf{s}}(y, t) + \delta\mathbf{s}(y, t, t_0) \quad (14)$$

into Eqs. (1)–(5), and linearization in  $\delta\mathbf{s}^0$  gives

$$\mathbf{A}(t_0, \eta, \xi)\delta\mathbf{s}^0 = \mathbf{0} \quad (15)$$

where

$$\mathbf{A}(t_0, \eta, \xi) = \begin{bmatrix} \rho\eta & -i\xi & -\ell\xi^2 & 0 & 0 \\ -is^0\xi & -1 & 0 & \eta + k\xi^2 & 0 \\ -\ell s^0\xi^2 & 0 & -1 & 0 & 0 \\ -is^0\xi & -1 & 0 & 0 & \left(1 + \frac{\psi^0}{\psi_0}\right)^n \eta \\ i\xi & -f_{,s}^0 & -f_{,\sigma}^0 & -f_{,\theta}^0 & -f_{,\psi}^0 \end{bmatrix}, \quad (16)$$

$f_{,s}^0 = \partial f^0 / \partial s|_{s=s^0}$  etc., and superscript zero on a variable signifies its value for the homogeneous solution at time  $t_0$ . The condition  $\det \mathbf{A} = 0$  yields the cubic equation

$$a\eta^3 + b\eta^2 + c\eta + d = 0 \quad (17)$$

for the growth rate  $\eta$ , where

$$\begin{aligned} a(t_0) &= \frac{\rho}{ms^0} \left(1 + \frac{\psi^0}{\psi_0}\right)^n, \\ b(\xi, t_0) &= \left(\frac{\ell^2}{m}\xi^4 + \left(1 + \frac{\rho k}{ms^0}\right)\xi^2 - \frac{\rho v}{m\theta^0}\right) \left(1 + \frac{\psi^0}{\psi_0}\right)^n + \frac{\rho n}{m\psi_0} \left(1 + \frac{\psi^0}{\psi_0}\right)^{-1}, \\ c(\xi, t_0) &= \left(\frac{\ell^2 k}{m}\xi^6 + \left(k - \frac{\ell^2 v s^0}{m\theta^0}\right)\xi^4 + \frac{v s^0}{m\theta^0}\xi^2\right) \left(1 + \frac{\psi^0}{\psi_0}\right)^n \\ &\quad - \frac{n}{m\psi_0} \left(1 + \frac{\psi^0}{\psi_0}\right)^{-1} (\ell^2 s^0 \xi^4 + (\rho k - s^0)\xi^2), \\ d(\xi, t_0) &= \frac{-n}{m\psi_0} \left(1 + \frac{\psi^0}{\psi_0}\right)^{-1} s^0 k (\ell^2 \xi^6 - \xi^4). \end{aligned} \quad (18)$$

For given values of  $t_0$  and  $\xi$ , Eq. (17) will have one real and two complex roots,  $\eta_i(\xi, t_0)$ ,  $i = 1, 2, 3$ . The root with the largest positive real part will govern the instability of the homogeneous solution, and is hereafter referred to as the dominant instability mode. For fixed  $t_0$ , one can compute the dominant instability mode as a

function of the wave number  $\xi$  and find the supremum,  $\eta_m$ , of the real parts of the roots of Eq. (17); henceforth we denote the wave number corresponding to  $\eta_m$  by  $\xi_m$ . Clearly,  $\eta_m$  and  $\xi_m$  are functions of  $t_0$ .

Using Wright and Ockendon's (1996) postulate that the wavelength of the dominant instability mode with the maximum growth rate at time  $t_0$  determines the shear band spacing  $L_s$ , we have

$$L_s = 2\pi/\xi_m(t_0^m), \quad (19)$$

where  $t_0^m$  corresponds to the time when  $\eta_m(t_0)$  is maximum. Molinari studied power-law type strain-hardening materials and found that

$$L_s = \inf_{t_0 \geq 0} \frac{2\pi}{\xi_m(t_0)} \quad (20)$$

gives essentially the same value as Eq. (19). Batra and Chen (1999) found that Eqs. (19) and (20) give quite different results when thermal softening of the material is described by an affine function of the temperature rise.

For locally adiabatic deformations of a nonpolar thermoviscoplastic material,  $\ell = 0$ ,  $k = 0$ . In this case  $d = 0$ , and Eq. (17) reduces to a quadratic equation in  $\eta$  whose both solutions are real and the positive solution is a monotonically increasing function of  $\xi$ . Thus for  $\ell = 0$  and  $k = 0$ , we have  $L_s = 0$ . A similar result was obtained by Batra and Chen (1999) for non-strain-hardening ( $n = 0$ ) thermoviscoplastic materials.

### 3.1. Results for CRS 1018 steel

We assigned the following values in *SI* units to the material parameters for the CRS 1018 steel studied by Molinari (1997).

$$\begin{aligned} \hat{\rho} &= 7800 \text{ kg/m}^3, m = 0.019, \nu = -0.38, \hat{\mu}_0 = 334 \times 10^7, \\ \hat{c} &= 500 \text{ J/kgK}, \hat{k} = 50 \text{ W/mK}, \hat{\kappa}_0 = 405 \text{ MPa}, \ell = 0.001, n = 0.015, \\ \psi_0 &= 0.01, \dot{\gamma}_0 t = 10^4/s, \bar{\psi}(0) = 0, \hat{\theta}_i = 300 \text{ K}, H = 2.5 \text{ mm}. \end{aligned} \quad (21)$$

Values of material parameters except for  $\ell$  are the same as those used by Molinari (1997); that for  $\ell$  is somewhat arbitrarily chosen,  $\psi_0$  is set equal to his prestrain  $\gamma_i$ , and  $\hat{\mu}_0 = \hat{\mu}_{0\text{molinari}}(\psi_0)^n$ . The effect of  $\ell$  on the shear band spacing is discussed below. Results presented herein are for a layer of *infinite* thickness, thus the effect of boundary conditions is not considered. The value of  $H$  is used to nondimensionalize the variables, and the homogeneous solution (12) is used to compute numerical results. When conducting parametric studies, values used of all parameters except the one being varied are those given in (21).

Fig. 1 depicts for homogeneous deformations of the body the shear stress  $s$  vs the work hardening parameter  $\psi$ , for  $n = 0, 0.015$  and  $0.1$ . When there is no work

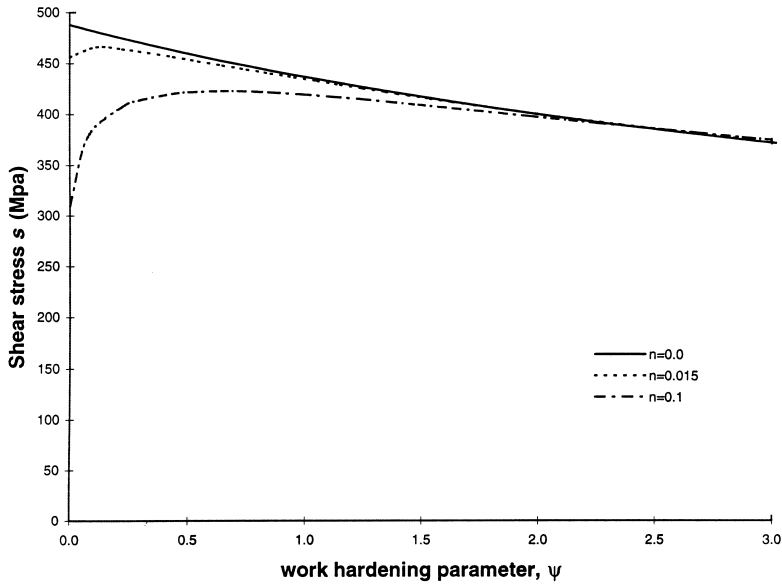


Fig. 1. Shear stress vs the work hardening parameter  $\psi$  for homogeneous simple shearing deformations of a thermoviscoplastic block.

hardening, i.e.  $n = 0$ , the stress decreases monotonically. However, when work hardening effects are considered, the value of  $\psi$  when the stress attains its maximum value increases with an increase in the value of the work hardening exponent  $n$ . Fig. 2 shows the growth rate  $\eta$  at time  $t_0$  or average strain  $\gamma_0$  vs the wave number  $\xi$  for six different values of the average strain  $\gamma_0$  when the initial perturbation is introduced. For each value of  $\gamma_0$ , the initial growth rate  $\eta$  first increases with  $\xi$ , attains a maximum value and then decreases; henceforth we call the maximum value  $\eta_m$  of  $\eta$  the dominant or the critical growth rate, and denote the corresponding wave number by  $\xi_m$ . As noted earlier,  $\eta_m$  and  $\xi_m$  depend upon  $\gamma_0$  or equivalently  $t_0$ , and  $\eta_m$  is not a monotonically increasing function of  $t_0$ . Figs. 3a and b exhibit, for four different values of the material characteristic length  $\ell$ , the dependence of  $\eta_m$  and the corresponding wavelength  $L_m = 2\pi/\xi_m$  upon the nominal strain  $\gamma_0$  when the perturbation is introduced. For each value of  $\ell$ ,  $\eta_m$  is maximum at  $\gamma_0 \simeq 0.5$ , but  $L_m$  is minimum for a little smaller value of  $\gamma_0$ . Molinari studied nonpolar ( $\ell = 0$ ) materials only and assumed that these two values of  $\gamma_0$  are the same. Whereas the hardening of the material due to its plastic deformations depends upon the plastic work done in our constitutive hypothesis (7), it depends on the plastic strain in the constitutive relation used by Molinari (1997). The values  $\gamma_0^m$  of  $\gamma_0$  corresponding to the maximum of  $\eta_m$  or the minimum of  $L_m$  equal about twice of that ( $\tilde{\gamma}_0$ ) where the stress attains its maximum value (cf. Fig. 1b) in the homogeneous solution. Note that the curves of  $L_m$  vs  $\gamma_0$  near the infimum of  $L_m$  are nearly flat. When thermal softening is modeled by an affine function of temperature, the infimum of  $L_m(t_0)$  occurs for a rather large value of  $t_0$  (e.g. see Batra and Chen (1999)). The values of the shear band spacing

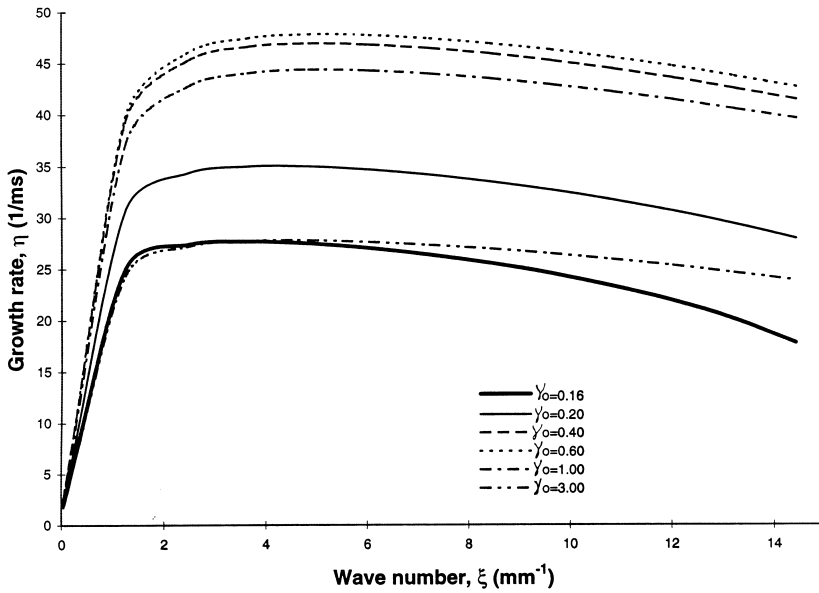


Fig. 2. Initial growth rate  $\eta$  vs the wave number  $\xi$  for six different values of the average strain,  $\gamma$ .

found by using Eqs. (19) and (20) and the plots in Figs. 3a and b are essentially equal to each other; values of the shear band spacing given below have been computed by using Eq. (20).

We have plotted in Fig. 4 the shear band spacing and the maximum initial growth rate as a function of the material characteristic length  $\ell$ . With an increase in the value of  $\ell$ , the maximum initial growth rate decreases gradually but the shear band spacing increases from 1.05 mm for  $\ell = 0$  to 3.4 mm for  $\ell = 0.01$ . The higher values of  $\ell$  increase the stabilizing effect of the dipolar theory, and increase the shear band spacing. Batra and Kim (1988) numerically studied the initiation and development of shear bands in dipolar thermoviscoplastic materials and found that the band width and the average strain at which a shear band initiated increase with an increase in the value of  $\ell$ . Nesterenko et al. (1995) observed  $\hat{L}_s = 0.85$  mm during the radial collapse of a thick-walled austenitic stainless steel cylinder deformed at a strain-rate of about  $10^4/s$ , and values obtained from Wright and Ockendon’s (1996) and Grady and Kipp’s (1987) models are (see Nesterenko et al., 1995)

$$\hat{L}_{WO} = 0.33 \text{ mm}, \hat{L}_{GK} = 1.8 \text{ mm}. \tag{22}$$

For the CRS 1018 steel with material properties given in (21), Molinari (1997) computed  $\hat{L}_s = 1.4$  mm. The difference between the presently computed value of  $\hat{L}_s$  and that obtained by Molinari (1997) is due to the different way of modeling the hardening of the material caused by plastic deformations. Wright and Ockendon

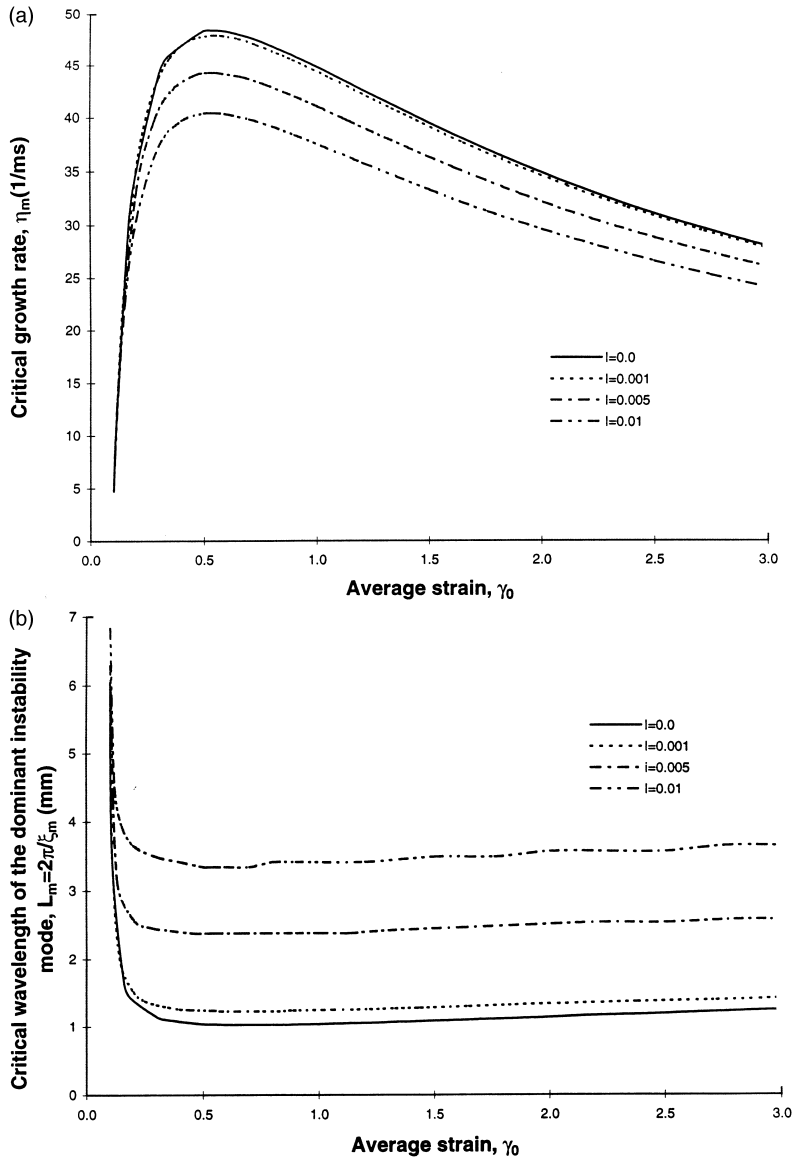


Fig. 3. Dependence of the maximum initial growth rate  $\eta_m$  and the corresponding wavelength  $L_m = 2\pi/\xi_m$  upon the nominal strain  $\gamma_0$  when the perturbation is introduced.

(1996) did not consider strain hardening of the material, and Grady and Kipp (1987) considered only thermal softening. It is not clear which microstructural parameters (e.g. grain size) determine the value of the material characteristic length. The present results suggest that the consideration of the microstructural effects significantly influences macroscopic phenomenon.

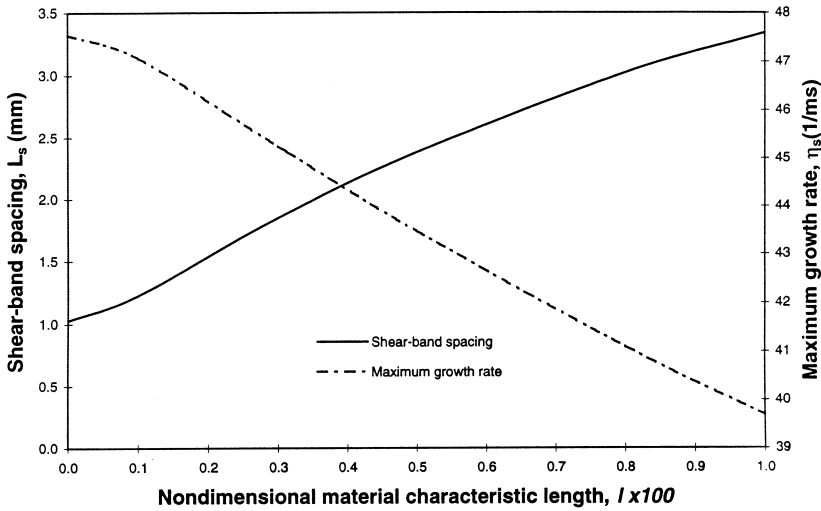


Fig. 4. Dependence of the shear band spacing and the maximum initial growth rate upon the material characteristic length  $\ell$ .

For a layer of finite thickness  $2H$ , the only admissible modes that satisfy the boundary conditions at  $y = \pm H$  are  $\xi_n = n\pi/H, n = 1, 2, \dots$ . Molinari (1997) has estimated the error caused by neglecting the effect of boundary conditions to be  $\hat{L}_s/2H$ . For the problem studied herein with  $\ell = 0, \hat{L}_s/2H = 0.21$ , the shear band spacing can vary from 0.84 to 1.26 mm. In the dipolar theory, one can determine  $\ell$  by matching the computed shear band spacing with the observed one. The validity of the dipolar theory then depends upon a favorable comparison of the computed and test results for other loadings.

Figure 5a evinces the effect of the work hardening exponent  $n$  upon the shear band spacing and the maximum initial growth rate. The shear band spacing increases and the maximum initial growth rate decreases monotonically with an increase in the value of  $n$ . The latter trend signifies the stabilizing effect of work hardening upon thermomechanical deformations of the viscoplastic body. Results plotted in Fig. 5b reveal that the average strain corresponding to the shear band spacing increases significantly as  $n$  is increased. Figures 6–9 exhibit the dependence of the shear band spacing, the maximum initial growth rate, and the nominal strain corresponding to the shear band spacing upon strain-rate hardening exponent  $m$ , thermal-softening exponent  $\nu$ , thermal conductivity  $k$ , and the nominal strain-rate  $\dot{\gamma}_0$ . The shear band spacing increases monotonically with an increase in the values of  $m$  and  $k$ , but  $L_s$  first decreases and then increases with an increase in the magnitude of the thermal softening coefficient. A five-fold change in the value of  $\hat{k}$  from 50 to 250 W/mK increases  $\hat{L}_s$  from 1.04 to 1.63 mm. However, a five-fold increase in the value of  $m$  from 0.02 to 0.10 enhances the value of  $\hat{L}_s$  from 1.4 to 2.9 mm. The average strain corresponding to the shear band spacing decreases with an increase in the value of  $m$  but increases with an increase in the absolute value of the thermal softening coeffi-

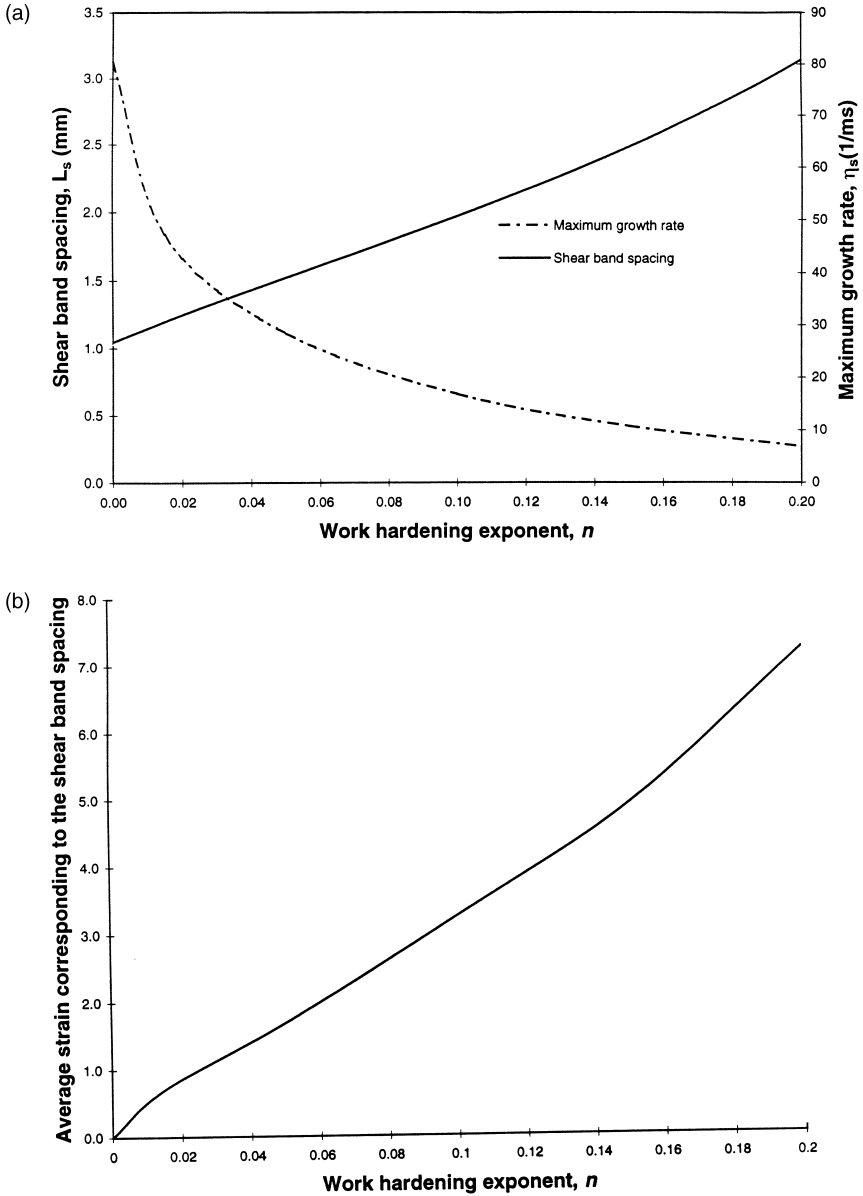


Fig. 5. (a) Dependence of the shear band spacing and the maximum initial growth rate upon the work hardening exponent  $n$ ; (b) effect of the work hardening exponent on the average strain corresponding to the shear band spacing.

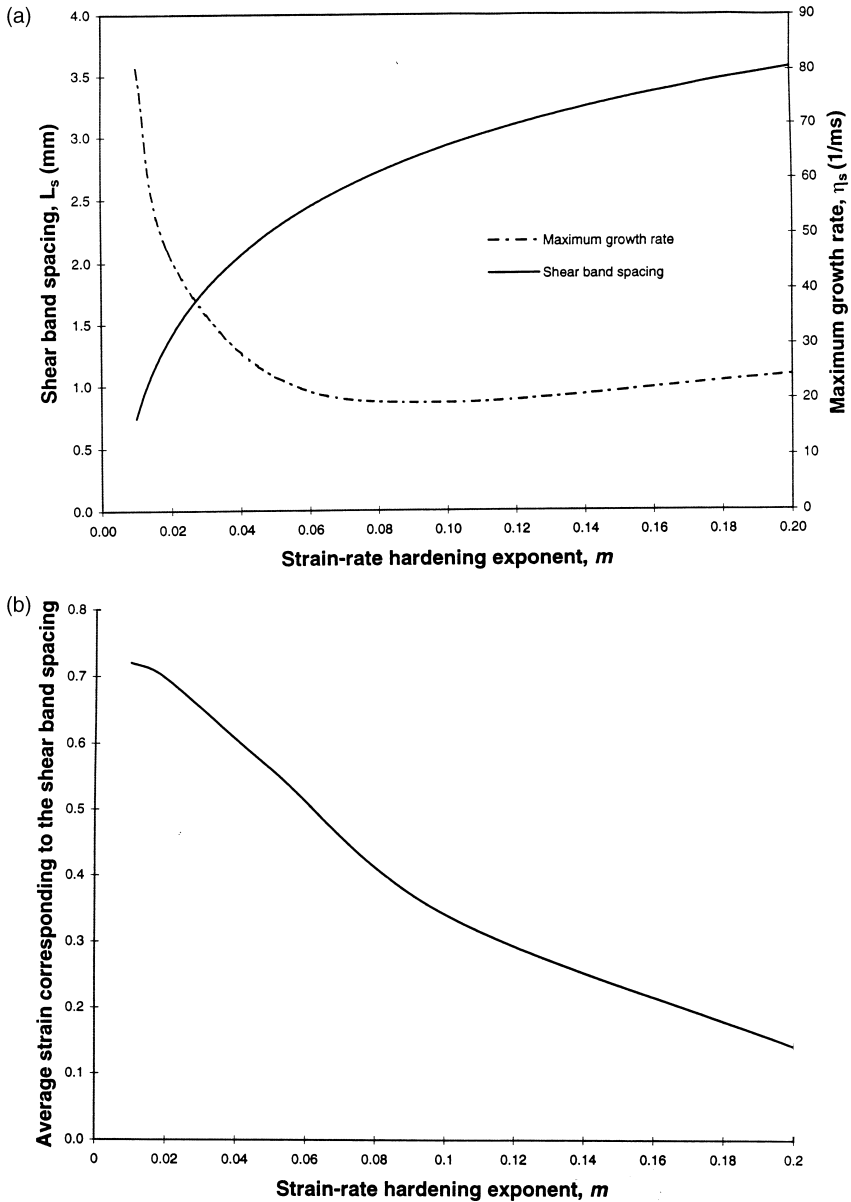


Fig. 6. (a) Dependence of the shear band spacing and the maximum initial growth rate upon the strain-rate hardening exponent  $m$ ; (b) effect of the strain-rate hardening exponent on the average strain corresponding to the shear band spacing.

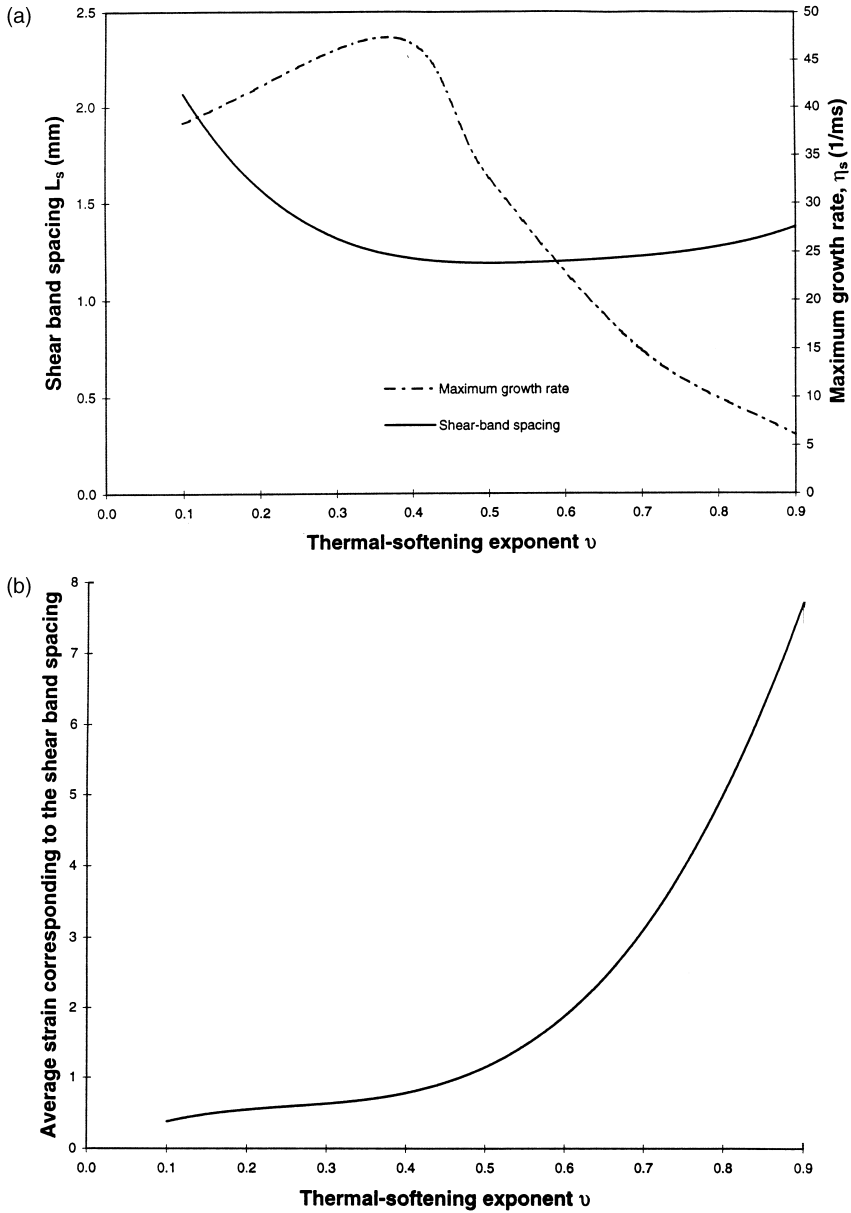


Fig. 7. (a) Dependence of the shear band spacing and the maximum initial growth rate upon the magnitude of the thermal softening exponent  $\nu$ ; (b) effect of the thermal-softening exponent on the average strain corresponding to the shear band spacing.

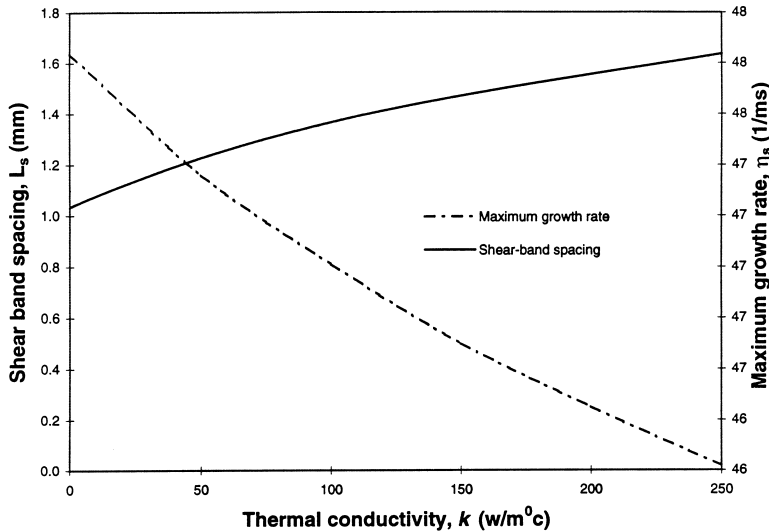


Fig. 8. Dependence of the shear band spacing and the maximum initial growth rate upon the thermal conductivity  $k$ .

cient. An explanation of the results plotted in Figs. 5b, 6b and 7b can be obtained by looking closely at the shear stress–shear strain curves for the homogeneous solution of the problem. Figures 10a–c depict the stress–strain curves for different values of  $m$ ,  $n$  and  $\nu$ . As  $|\nu|$  and  $n$  increase, the shear stress vs the average strain curves beyond the peak in the shear stress become flat,  $|ds/d\gamma|$  at a fixed value of  $\gamma$  decreases, and the stress drops rather slowly with an increase in the average strain. However, with increasing  $m$ ,  $|ds/d\gamma|$  at a fixed value of  $\gamma$  increases. Thus the average strain corresponding to the shear band spacing seems to depend upon the rate of drop of the shear stress in the homogeneous solution. For the range of values of  $\hat{k}$  considered, the nominal strain corresponding to the shear band spacing was virtually unaffected by the value of  $\hat{k}$ . Note that  $\hat{k}$  and  $\hat{\ell}$  do not appear in the homogeneous solution of the problem. Results plotted in Fig. 9b reveal that the average strain corresponding to the initiation of the shear band spacing first decreases with an increase in the value of the nominal strain-rate from 100/s to  $2 \times 10^4$ /s and then increases. Wright and Walter (1987) neglected the work-hardening of the material and obtained a U shape curve for the average strain at the initiation of an instability vs the nominal strain-rate. Our results show that beyond a nominal strain-rate of  $3 \times 10^4$ /s, the average strain corresponding to the shear band spacing and also to the initiation of an instability is essentially unaltered by the nominal strain-rate. It should be noted that the results depend upon the constitutive relation employed, and Wright and Walter (1987) modeled thermal softening by an affine function of the temperature rise.

For the material parameters used by Kwon and Batra (1988) with affine thermal softening and average strain-rate of  $5 \times 10^4$ /s, definition (20) of the shear band spacing gives  $\hat{L}_s = 0.294, 0.32$  and  $0.68$  mm for  $\ell = 0, 0.001$  and  $0.01$ , respectively;

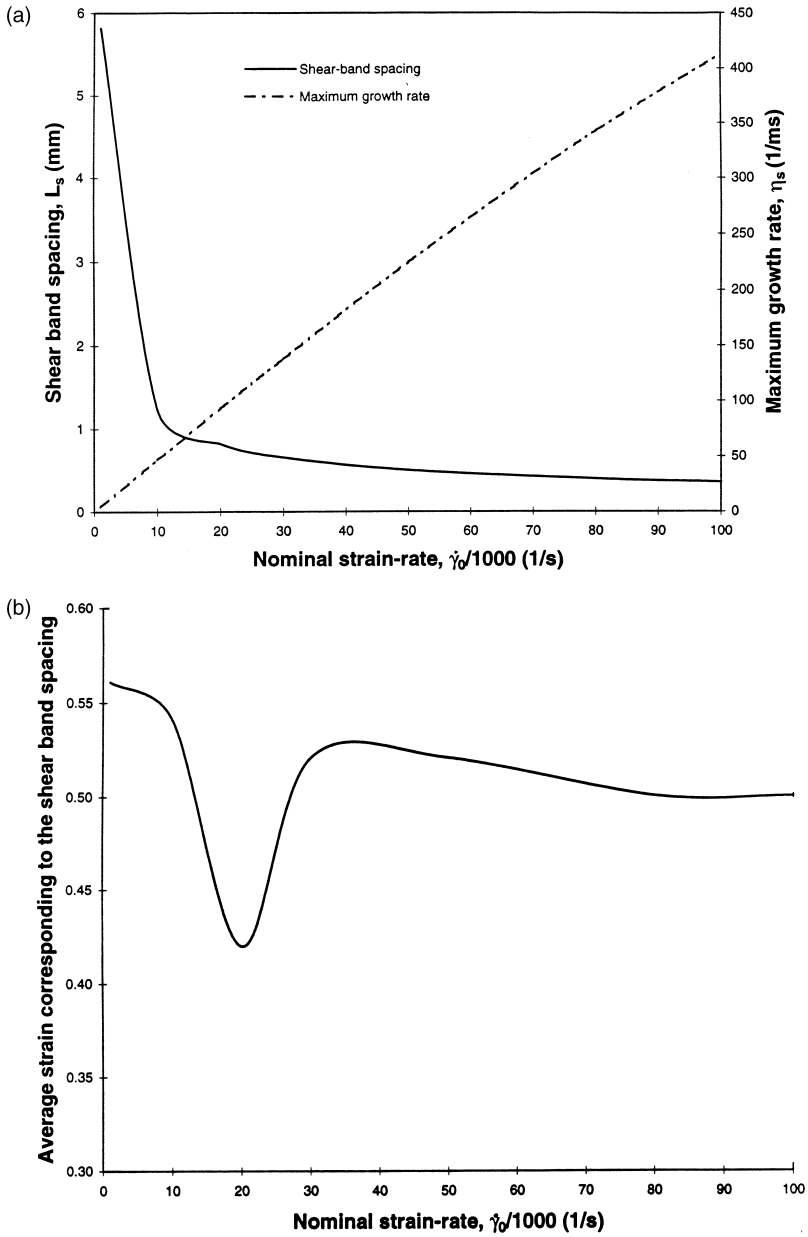


Fig. 9. (a) Dependence of the shear band spacing and the maximum initial growth rate upon the nominal strain-rate; (b) effect of the nominal strain-rate on the average strain corresponding to the shear band spacing.

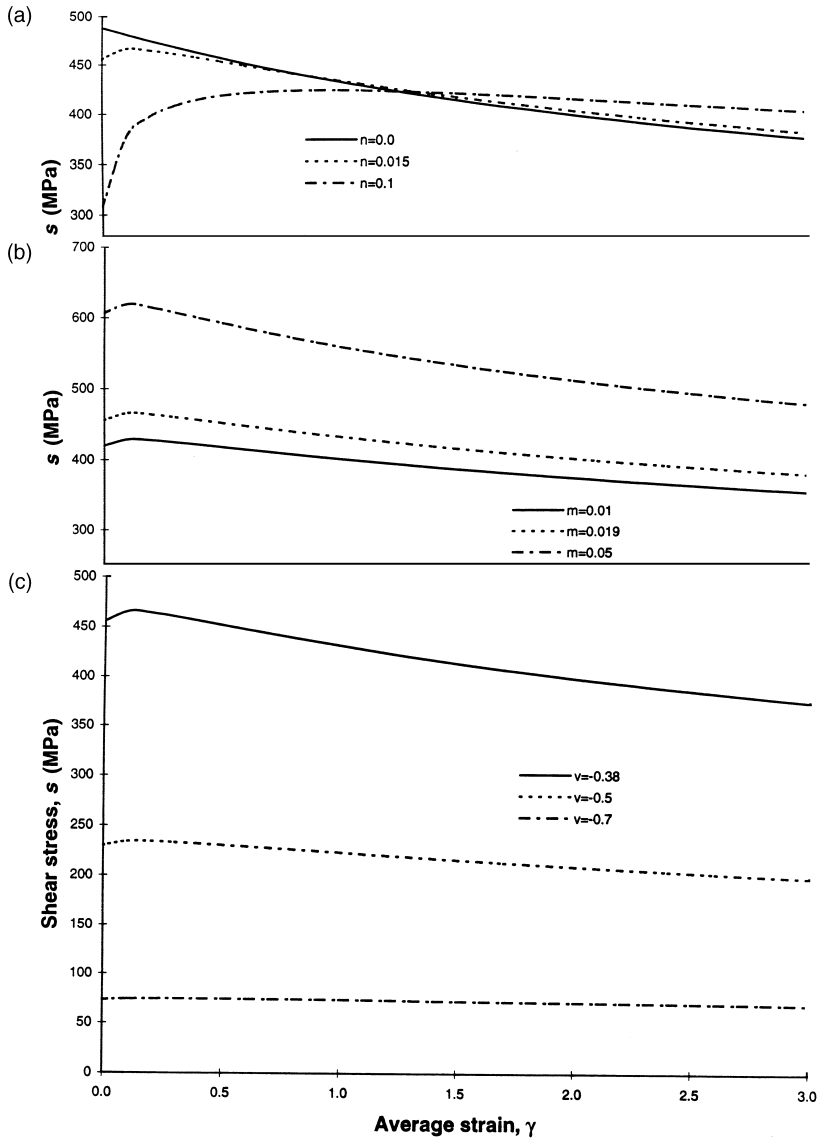


Fig. 10. Shear stress–shear strain curves for the homogeneous solution for different values of (a)  $m$ , (b)  $n$ , and (c)  $\nu$ .

corresponding values obtained from definition (19) are 1.73, 1.94 and 6.0 mm. Kwon and Batra's (1999) numerical solution yielded the same value of  $\hat{L}_s \leq 0.258$  mm for  $\ell = 0$  and 0.01. They considered the effect of material elasticity and boundary conditions, and solved the complete set of coupled nonlinear partial differential equations, and did not find the minimum value of the shear band spacing.

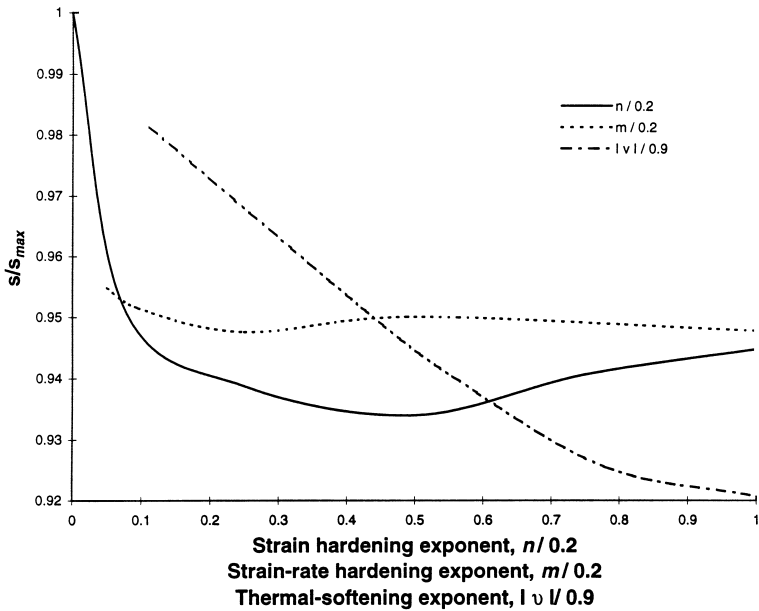


Fig. 11. Dependence of  $\bar{s}/s_{max}$  upon various material parameters. Here  $\bar{s}$  equals the value of the shear stress when perturbations of minimum wavelength begin to grow predominantly.

Batra and Kim (1992) conducted numerical experiments on the initiation and development of shear bands in twelve materials and modeled the thermoviscoplastic response of these materials by the Johnson–Cook (1983) relation which represents thermal softening by an affine function of temperature rise. They concluded that a shear band begins to grow in earnest when the shear stress has dropped to nearly 90% of its maximum value. In order to examine how this value correlates with the average strain  $\gamma_0^m$  or time  $t_0^m$  corresponding to the infimum of  $L_m(t_0)$ , we have plotted in Fig. 11  $\bar{s}/s_{max}$  vs  $m$ ,  $n$  and  $\nu$ , where  $\bar{s}$  equals the value of  $s$  at an average strain of  $\gamma_0^m$  in the homogeneous solution. For a large range of values of  $m$ , the perturbation introduced when  $\bar{s}/s_{max} \equiv 0.955$  yields the shear band spacing. However,  $\bar{s}/s_{max}$  decreases from 0.98 to 0.92 as  $|\nu|$  increases from 0.09 to 0.9. The decrease in  $\bar{s}/s_{max}$  is quite sharp when  $n$  is increased from 0 to 0.02 but  $\bar{s}/s_{max} \approx 0.94$  for  $0.2 \geq n \geq 0.02$ . As noted earlier, for the affine thermal softening, the shear band spacing corresponds to perturbations introduced at a much larger value of  $\gamma_0$  or a smaller value of  $\bar{s}/s_{max}$  as compared to that for a power law material.

#### 4. Approximate expressions for shear band spacing

The following analysis follows closely Molinari's (1997) work. The numerical results presented above indicate that for given  $\xi$  and  $t_0$ , (17) always has a root with a positive real part. For a fixed  $t_0$ ,  $\eta$  assumes a maximum value at the wave number  $\xi_m$ . Therefore,

$$\left. \frac{\partial \eta(\xi, t_0)}{\partial \xi} \right|_{\xi=\xi_m} = 0. \tag{23}$$

We first consider locally adiabatic deformations, i.e.  $k = 0$  and determine an approximate expression for the shear band spacing in thermoviscoplastic materials characterized by (7). Differentiating (17) with respect to  $\xi$ , evaluating the result at  $\xi = \xi_m$  and using (23) we obtain

$$b'_m \eta_m + c'_m = 0 \tag{24}$$

where

$$b'_m = \left. \frac{\partial b(\xi, t_0)}{\partial \xi} \right|_{\xi=\xi_m}, \quad c'_m = \left. \frac{\partial c(\xi, t_0)}{\partial \xi} \right|_{\xi=\xi_m}, \tag{25}$$

$b$  and  $c$  are given by (18). Evaluating (17) at  $\eta = \eta_m$  and  $\xi = \xi_m$ , and eliminating  $\eta_m$  from it and (24), we arrive at

$$a(c'_m)^2 - b_m b'_m c'_m + c_m (b'_m)^2 = 0, \tag{26}$$

where  $b_m = b(\xi_m, t_0)$ ,  $c_m = c(\xi_m, t_0)$ .

The left-hand side of Eq. (26) is a polynomial of degree 12 in  $\xi_m$  with coefficients depending upon  $t_0$  since  $s^0$ ,  $\theta^0$  and  $\psi^0$  are functions of  $t_0$ . Estimating the order of magnitude of each term in Eq. (26), noting that  $\ell \ll 1$ , and retaining only the dominant terms, we get

$$\xi_m = \left( \frac{\rho}{m \ell^2} \right)^{1/4} \left[ -\frac{\nu}{\theta^0} - \frac{n}{\psi_0} \frac{1}{\left( 1 + \frac{\psi^0}{\psi_0} \right)^{1+n}} \right]^{1/4}. \tag{27}$$

Evaluating (12) at  $t = t_0$ , substituting for  $\psi^0$  in terms of  $\theta^0$ , recalling that  $L_m = 2\pi/\xi_m$ , and using (6), we obtain

$$\hat{L}_m(t_0) = 2\pi \left( \frac{\hat{\ell}}{\hat{\gamma}_0} \right)^{1/2} (m\hat{c})^{1/4} \left[ -\frac{\nu}{\hat{\theta}^0} - \frac{n}{(1+n)(\hat{\theta}^0 - \hat{\theta}_0)} \right]^{-1/4}, \tag{28}$$

where  $\hat{\theta}_0 = \hat{\theta}(0) - \theta_r \frac{\psi_0}{1+n} \left( 1 + \frac{\bar{\psi}(0)}{\psi_0} \right)^{1+n}$ , and a superimposed hat indicates that the quantity is expressed in SI units. When  $n = 0$ , expression (28) reduces to Eq. (40) of Batra and Chen (1999). For  $\theta_0 = 0$  and  $|\nu| > n/(1+n)$ , it follows from Eq. (28) that  $\hat{L}_m(t_0)$  is minimum at  $t_0 = 0$  since  $\hat{\theta}^0$  is a monotonically increasing function of  $t_0$ .

Eq. (28) and  $d\hat{L}_m/dt_0 = 0$  give

$$\hat{\theta}^0(t_0^m) = \hat{\theta}_0/[1 - (-\nu/\tilde{n})^{-1/2}] \tag{29}$$

where  $t_0^m$  corresponds to the time when  $\hat{L}_m(t_0)$  takes on an extreme value. Equations (12) and (29) show that  $t_0^m$  is unaffected by the value of  $\ell$  which also could be concluded from the results plotted in Fig. 3a. Substitution from (29) into (28), and using definition (20) of the shear band spacing results in the expression,

$$\hat{L}_s = 2\pi \left(\frac{\hat{\ell}}{\dot{\gamma}_0}\right)^{1/2} \left(\frac{m\hat{c}\hat{\theta}_0}{(1 - (-\nu/\tilde{n})^{-1/2})}\right)^{1/4} (-\nu)^{-1/8} [(-\nu)^{1/2} - (\tilde{n})^{1/2}]^{-1/4}, \tag{30}$$

for the minimum spacing among adiabatic shear bands. For the shear band spacing to be positive,  $|\nu| > \tilde{n}$ . Thus the critical shear band spacing in locally adiabatic deformations of a strain-hardening dipolar viscoplastic material depends upon the square-root of the material characteristic length, fourth-root of the strain-rate hardening exponent, and the negative square-root of the nominal strain-rate. Figure 12 shows a comparison of the shear band spacing as a function of the material characteristic length as computed from the definition (20) with the numerical solution of the homogeneous problem, and the approximate relation Eq. (30). It is clear that (30) gives very good values of the shear band spacing.

We now derive an approximate expression for the shear band spacing in heat conducting nonpolar ( $\ell = 0$ ) thermoviscoplastic materials. With the assumptions  $m \ll 1, \rho k f_{,s} \ll 1, \rho k \ll s$ , expressions (18) for  $b, c$  and  $d$  can be approximated as follows.

$$\begin{aligned} b &\simeq \left(1 + \frac{\psi^0}{\psi_0}\right)^n \left(\xi^2 - \frac{\rho\nu}{m\theta^0}\right) - \frac{\rho n}{m\psi_0} \left(1 + \frac{\psi^0}{\psi_0}\right)^{-1}, \\ &\equiv b_0 \xi^2 + b_1, \\ c &\simeq k \left(1 + \frac{\psi^0}{\psi_0}\right)^n \xi^4 + \left(\frac{\nu s^0}{m\theta^0} \left(1 + \frac{\psi^0}{\psi_0}\right)^n + \frac{ns^0}{m\psi_0} \left(1 + \frac{\psi^0}{\psi_0}\right)^{-1}\right) \xi^2, \\ &\equiv c_0 \xi^4 + c_1 \xi^2, \\ d &= \frac{nk s^0}{m\psi_0} \left(1 + \frac{\psi^0}{\psi_0}\right)^{-1} \xi^4 \equiv d_0 \xi^4 \end{aligned} \tag{31}$$

Substitution from (17), (18)<sub>1</sub> and (31) into (23) yields

$$b_0 \eta_m^2 + (c_1 + 2c_0 \xi_m^2) \eta_m + 2d_0 \xi_m^2 = 0 \tag{32}$$

whose approximate solution is

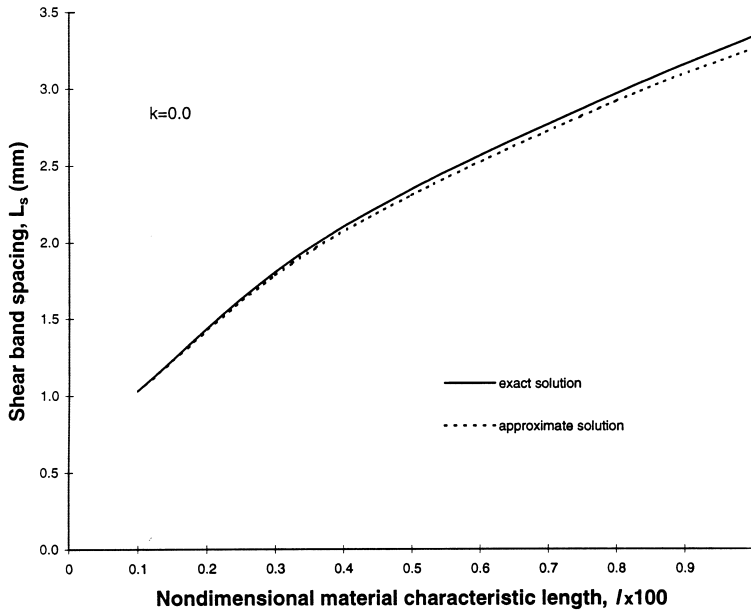


Fig. 12. Comparison of the shear band spacing as a function of the material characteristic length as computed from the numerical solution of the complete set of equations and the approximate relation (30).

$$\eta_m \simeq -\frac{c_1 + 2c_0\xi_m^2}{b_0} + \frac{2d_0\xi_m^2}{c_1 + 2c_0\xi_m^2}. \tag{33}$$

Substituting from (33) into (17), estimating the order of magnitude of each term and retaining only the dominant terms, we obtain

$$A\xi_m^4 + B\xi_m^2 + C = 0 \tag{34}$$

where

$$\begin{aligned} A &= (c_0c_1/b_0) - d_0, \\ B &= 6ac_1(d_0 - c_0c_1b_0)/b_0^2, \\ C &= -ac_1^3/b_0^3. \end{aligned} \tag{35}$$

Equation (34) can be solved for  $\xi_m^2$  and then  $\eta_m$  can be computed from (33). Since coefficients  $a, b_0, c_0, d_0, b_1$  and  $c_1$  depend upon  $t_0$ ,  $\xi_m^2$  computed from (34) is a function of  $t_0$ . The expression for  $t_0^m$  that makes  $\xi_m$  maximum is very involved. However,  $\xi_m$  can be plotted as a function of  $t_0$  and the maximum value of  $\xi_m$  and the shear band spacing determined.

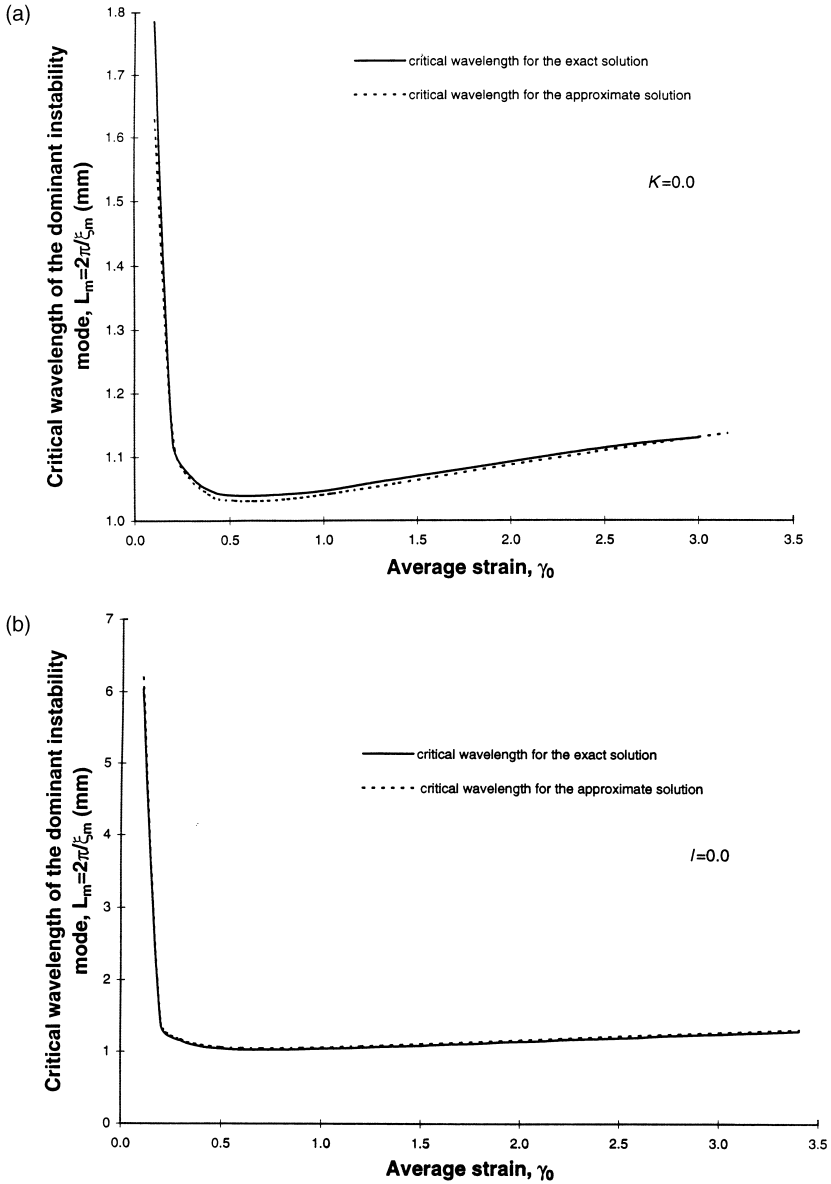


Fig. 13. Comparison of the dependence of the critical wavelength of the dominant instability mode upon the nominal strain as computed from the approximate analytic expression and the solution of the complete set of equations (a)  $k = 0$ , (b)  $l = 0$ .

Figs. 13a and b compare the dependence of the critical wavelength of the dominant instability mode upon the nominal strain as computed from (28) and (34) with those obtained from a solution of the complete set of equations. A close agreement between the two sets of results indicates that the assumptions made in deriving (28) and (34) are reasonable.

## 5. Conclusions

We have ascertained shear band spacing in strain-rate gradient-dependent, work-hardening, strain-rate hardening and thermally softening viscoplastic materials undergoing simple shearing deformations. Higher-order stresses corresponding to the strain-rate gradients are included in the governing equations and the yield function. A homogeneous solution of the governing equations is perturbed at different times  $t_0$  and the growth rate at  $t_0$  of perturbations is computed as a function of the wave number. The wavelength of the dominant mode of instability with the maximum growth rate at  $t_0$  is assumed to determine the shear band spacing. The shear band spacing rapidly increases with an increase in the work-hardening exponent and in the material characteristic length. It also increases with a rise in the value of the thermal conductivity and the strain-rate hardening exponent. The average strain  $\gamma_0$  corresponding to the shear band spacing correlates well with the rate of drop of the shear stress in the homogeneous solution; higher values of  $\gamma_0$  correspond to the slower rate of drop of the shear stress. Approximate analytic expressions for the shear band spacing in locally adiabatic deformations of dipolar thermoviscoplastic materials indicate that the shear band spacing varies as the square-root of the material characteristic length, fourth-root of the strain-rate hardening exponent, and negative square-root of the average or nominal strain-rate. The effects of the thermal softening and the work-hardening exponents are inter-related. When work-hardening of the material can be neglected, then the shear band spacing varies as the negative fourth-root of the thermal softening exponent.

## Acknowledgement

This work was supported by the ONR grant N00014-98-1-0300 to Virginia Polytechnic Institute and State University with Dr. Y.D.S. Rajapakse as the program manager.

## References

- Aifantis, E.C., 1984. On the microstructural origins of certain inelastic models. *J. Eng'g. Mat. Tech.* 106, 326–330.
- Anand, L., Kim, K.H., Shawki, T.G., 1987. Onset of shear localization in viscoplastic solids. *J. Mech. Phys. Solids* 35, 427–429.

- Bai, Y.J., 1982. Thermo-plastic instability in simple shear. *J. Mech. Physics of Solids* 30, 195–207.
- Bai, Y.L., Dodd, B., 1992. *Adiabatic Shear Localization: Occurrence, Theories and Applications*. Pergamon, Oxford.
- Batra, R.C., 1975. On heat conduction and wave propagation in non-simple rigid solids. *Letters in Appl. & Eng'g. Sci.* 3, 97–107.
- Batra, R.C., 1987. The initiation and growth of, and the interaction among adiabatic shear bands in simple and dipolar materials. *Int. J. Plasticity* 3, 75–89.
- Batra, R.C. and Chen, L., Shear band spacing in gradient-dependent thermoviscoplastic materials. *Computational Mech.* in press.
- Batra, R.C., Hwang, J., 1994. Dynamic shear band development in dipolar thermoviscoplastic Materials. *Computational Mech.* 12, 354–369.
- Batra, R.C., Kim, C.H., 1988. Effect of material characteristic length on the initiation, growth and band width of adiabatic shear bands in dipolar materials. *J. Physique* 49 (C3), 41–46.
- Batra, R.C., Kim, C.H., 1990. Adiabatic shear banding in elastic-viscoplastic nonpolar and dipolar materials. *Int. J. Plasticity* 6, 127–141.
- Batra, R.C., Kim, C.H., 1992. Analysis of shear bands in twelve materials. *Int. J. Plasticity* 8, 425–452.
- Burns, T.J., 1985. Approximate linear stability analysis of a model of adiabatic shear band formation. *Q. Appl. Math.* 43, 65–84.
- Clifton, R.J., 1980. Adiabatic shear in material response to ultrahigh loading rates. Report no. NMAB-356. National Materials Advisory Board Committee, pp.129–142. (Chapter 8).
- Faci, C., Molinari, A., 1996. Evolution of layered structures in a gradient-dependent viscoplastic material. *J. de Physique IV* 6 (C1), 45–54.
- Faci, C., Molinari, A., 1998. A non-local rate-type viscoplastic approach to patterning of deformation. *Acta Mechanica* 126, 71–99.
- Grady, D.E., Kipp, M.E., 1987. The growth of unstable thermoplastic shear with application to steady-wave shock compression in solids. *J. Mech. Phys. Solids* 35, 95–118.
- Johnson, G.R., Cook, W.H., 1983. A constitutive model and data for metals subjected to large strains, high strain rates and high temperatures. *Proc. 7th Int. Symp. Ballistics, The Hague*, pp. 1–10.
- Kwon, Y.W. and Batra, R. C., 1988. Effect of multiple initial imperfections on the initiation and growth of adiabatic shear bands in nonpolar and dipolar materials. *Int. J. Engng. Sci.* 26, 1177–1187.
- Molinari, A., 1985. Instabilité thermo-visco-plastique en cisaillement simple. *J. Méc. Theor. Appl.* 4, 659–684.
- Molinari, A., 1997. Collective behavior and spacing of adiabatic shear bands. *J. Mech. Phys. Solids* 45, 1551–1575.
- Nesterenko, V.F., Meyers, M.A., Wright, T.W., 1995. Collective behavior of shear bands. In: Murr, L.E., Staudhammer, K.P., Meyers, M.A. (Eds.), *Metallurgical and Materials Application of Shock-Wave and High-Strain-Rate Phenomena*. Elsevier Science, Amsterdam, pp. 397–404.
- Wright, T.W., Batra, R.C., 1987. Adiabatic shear bands in simple and dipolar plastic materials. In: Kawata, K., Shiori, J. (Eds.), *Macro- and Micro-Mechanics of High Velocity Deformation and Fracture*, IUTAM Symp. on MMMHVDF, Tokyo, Japan. Springer-Verlag, Berlin, Heidelberg, pp. 189–201.
- Wright, T.W., Ockendon, H., 1996. A scaling law for the effect of inertia on the formation of adiabatic shear bands. *Int. J. Plasticity* 12, 927–934.
- Wright, T.W., Walter, J.W., 1987. On stress collapse in adiabatic shear bands. *J. Mech. Phys. Solids* 35, 701–720.